lentiviruses was also measured, and there were no significant differences between R424H mutant-expressing and control cultures (GFP, 71.2 ± 41.2 nM, $n = 86$; WT, 69.7 ± 38.0 nM, $n = 118$; R424H, 63.6 ± 32.9 nM, $n = 72$; $P = 0.365$ between GFP and R424H; $P = 0.423$ between WT and R424H).

To examine whether the elevated basal $[Ca^{2+}]_i$ induced PC death in R424H mutant-expressing cultures, we performed a similar experiment to that in Fig. 2. In this experiment, ω-agatoxin IVA (0.2 μM) was added to the culture medium at DIV 2 (see Methods), and WT-expressing cultures were omitted to simplify the experimental design. Treatment of GFP-expressing cultures with ω-agatoxin IVA did not affect relative PC density (Fig. 9*D*, filled circles) but increased the branch number and the total length of dendrites at DIV 14 (Fig. 9*E* and *F*; filled circles in Fig. 9*I* and *J*), in good agreement with a previous report (Schilling *et al.* 1991; see Discussion). Treatment of R424H mutant-expressing cultures with ω-agatoxin IVA significantly increased relative PC density at DIV 11 and 14 (Fig. 9*D*, red triangles) and significantly rescued dendritic development in PCs (Fig. 9*G* and *H*; red triangles in Fig. 9*I* and *J*). These results clearly indicate that P/Q-type Ca^{2+} channels play a critical role in the PC death and impairment of dendrite development caused by R424H mutant expression, and support our hypothesis.

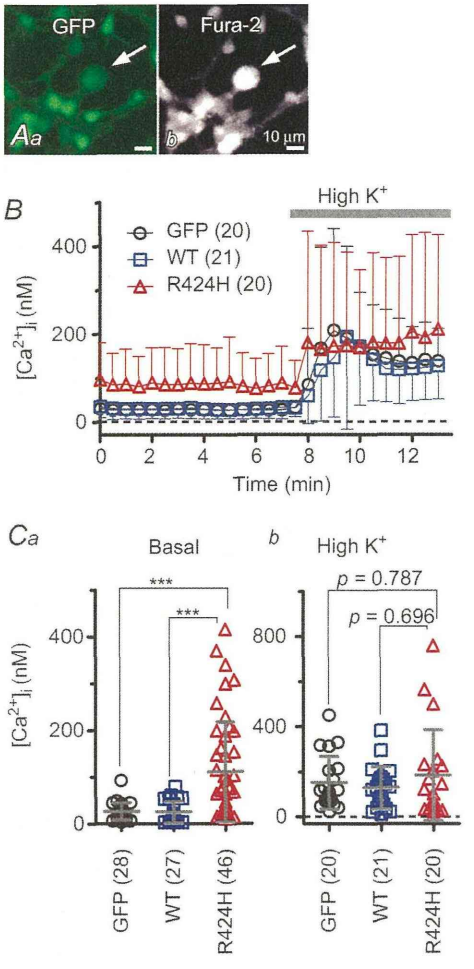

Figure 8. Significantly higher basal $[Ca^{2+}]_i$ in PCs expressing R424H mutant

A, representative fluorescence images of a fura-2 AM-loaded cerebellar culture expressing GFP alone. Arrows indicate PCs. *Aa*, GFP fluorescence (excitation, 470–495 nm; emission, 510–550 nm). *Ab*, fura-2 fluorescence (excitation, 375–385 nm; emission, 470–550 nm). *B*, the time course of free $[Ca^{2+}]_i$ in PCs. To depolarize PCs, high-K^+ ACSF (High K^+) was bath applied during the time indicated by the grey bar. *C*, summary of averaged $[Ca^{2+}]_i$ in PCs. Basal $[Ca^{2+}]_i$ was obtained as the average of a 7 min period from the beginning of the recordings (*Ca*), and elevated $[Ca^{2+}]_i$ from a 5 min period during high-K^+ ACSF perfusion (*Cb*). ***$P < 0.001$.

Discussion

In this study, we found that the expression of R424H mutant subunits in cerebellar cultures significantly impaired dendritic development and survival in PCs (Figs 2 and 3). Prior to cell death, R424H mutant-expressing PCs showed broadened action potential waveforms, altered firing properties and elevated basal $[Ca^{2+}]_i$ (Figs 6–8). Moreover, chronic inhibition of P/Q-type Ca^{2+} channels by ω-agatoxin IVA rescued the PC death and dendritic maldevelopment caused by expression of R424H mutant subunits (Fig. 9). This is the first report to show that a missense mutation found in SCA13 patients induces maldevelopment of PC dendrites and eventually PC death, most probably due to elevated basal $[Ca^{2+}]_i$ in PCs.

Biophysical properties of R424H mutant channels

The biophysical properties of hKv3.3 channels with the R423H mutation, which corresponds to the R424H mutation in mKv3.3 channels, have been previously reported (Figueroa *et al.* 2010; Minassian *et al.* 2012). Our results in Supplemental Fig. S2 agreed well with the previous reports and suggest that the properties of R424H mutant mKv3.3 were essentially identical to those of R423H-mutant hKv3.3. Moreover, we found that coexpression of R424H mutant and WT subunits accelerated the inactivation kinetics and slowed recovery from inactivation compared with expression of WT subunits alone (Fig. 1). Therefore, we predict that the properties we found in R424H mutant mKv3.3 are shared with R423H mutant hKv3.3.

We confirmed that homomeric R424H mutant channels showed negligible currents and that R424H mutant subunits exerted a dominant-negative influence on WT mKv3.3 channels in *Xenopus* oocytes (Supplemental Fig. S2*A* and *B*; Figueroa *et al.* 2010, 2011). Very recently,

Zhao *et al.* (2013) reported that in heterologous expression systems using Chinese hamster ovary cells, the surface protein level of R423H mutant hKv3.3 channels is 30% of that of WT hKv3.3 and that the conductance density of the mutant is 16% of that of the WT. Therefore, we cannot exclude the possibility that the reduced surface expression of mKv3.3 channels by the mutation would also contribute to the broadening of action potentials (Fig. 6) and lower firing frequency (Fig. 7) in transduced PCs. However, the reduction of the conductance density cannot be explained fully by the reduced surface protein expression.

To explain the negligible activity and dominant-negative property of R424H mutant channels, we propose two hypothetical mechanisms. First, the positively charged arginine at position 424 in mKv3.3 may be a critical residue in the S4 segment, serving as a part of the voltage sensor domain (Seoh *et al.* 1996). The partial disruption of the sensor domain by R424H mutation would make the subunits less sensitive to membrane voltage changes, resulting in the loss of channel function. Second, an arginine residue at position 174 in the S4 segment of KAT1, which is a voltage-gated K^+ channel in *Arabidopsis*, plays an essential role in the appropriate integration of the S3 and S4 segment into the endoplasmic reticulum membrane (Sato *et al.* 2003). Given that the R174 is homologous to R424 in mKv3.3, defective membrane insertion of R424H mutant subunits could occur in *Xenopus* oocytes, leading to a defect in channel activity.

Purkinje cell death by R424H mutant expression and the inhibition by blockade of P/Q-type voltage-gated Ca^{2+} channels

In this study, we revealed that expression of R424H mutant subunits caused cell death and impaired dendritic growth in PCs (Figs 2 and 3) and that these effects were reversed by the blockade of P/Q-type Ca^{2+} channels (Fig. 9). Addition of ω-agatoxin IVA also enhanced dendritic elongation in PCs expressing GFP alone (Fig. 9*E* and *F*; filled circles in Fig. 9*I* and *J*). Together with a previous report showing that chronic application of TTX in cerebellar cultures caused dendritic elongation in PCs (Schilling *et al.* 1991), activation of P/Q-type Ca^{2+} channels by neuronal activity may adversely influence dendritic elongation in PCs. Addition of ω-agatoxin IVA in R424H mutant-expressing cultures did not completely restore PC survival rates

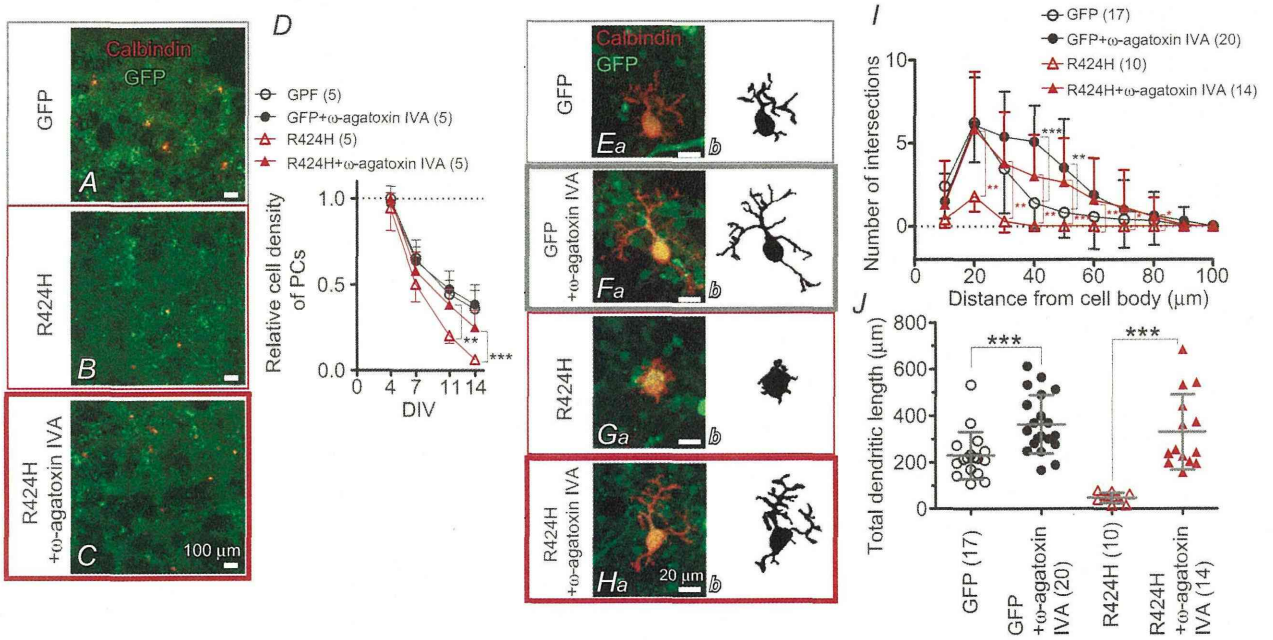

Figure 9. Pharmacological blockade of P/Q-type Ca^{2+} channels rescues the PC death and dendritic maldevelopment caused by expression of R424H mutant
A–C, cerebellar cultures expressing GFP alone (*A*) or R424H mutant with GFP (*B* and *C*). The cultures were immunostained for calbindin at DIV 14. In *C*, ω-agatoxin IVA was added to the culture medium every other day from DIV 2. *D*, relative cell density of PCs plotted as a function of DIV. The density was normalized to the value of PCs expressing GFP alone at DIV 4. *E–H*, calbindin-immunolabelled PCs expressing GFP alone (*Ea* and *Fa*) or R424H mutant subunits with GFP (*Ga* and *Ha*) at DIV 14. Morphologies of PCs are depicted in the right-hand panels for clarity. In *F* and *H*, ω-agatoxin IVA was added. *I*, and *J*, summary of dendrite complexity measured by Sholl analysis (*I*) and of total dendritic length (*J*). $^*P < 0.05$, $^{**}P < 0.01$, and $^{***}P < 0.001$.

(Fig. 9*D*). This may be because some Ca^{2+} currents in cultured PCs are mediated by Ca^{2+} channels other than the P/Q-type (Gillard *et al.* 1997), and activation of these channels may contribute to PC death. We therefore performed the same rescue experiments using $CdCl_2$ (0.2 mM; a non-selective Ca^{2+} channel blocker) or a combination of ω-agatoxin IVA and verapamil hydrochloride (0.02 mM; an L-type Ca^{2+} channel blocker), but these chemicals markedly deteriorated the viability and development of cerebellar cultures within 3 DIV (data not shown).

In contrast to PCs, there were no significant decreases in the numbers of granule cells upon R424H mutant expression (Fig. 2*E*). This may be because granule cells do not express endogenous mKv3.3 channels with which R424H mutant subunits form oligomeric channels (Supplemental Fig. S3*C*), resulting in the absence of the dominant-negative influence on the endogenous channels by the expression of mutant channel subunits.

Comparison with preceding papers on Kv3.3 knockout mice and zebrafish expressing mutant Kv3.3

In contrast to the impaired dendritic development in R424H mutant-expressing PCs (Fig. 3*Cb″* and *D*), the cerebellum of Kv3.3 knockout mice shows neither dendritic shrinkage of PCs nor cerebellar atrophy (Zagha *et al.* 2010). Furthermore, the knockout mice display only moderate motor dysfunction and no ataxic phenotype, although SCA13 patients show severe ataxia (Joho *et al.* 2006; Hurlock *et al.* 2008; Waters & Pulst, 2008; Figueroa *et al.* 2010). This difference may be attributable to the following factors. In PCs, mKv3.3 is thought to form heteromultimeric channels by assembling with Kv3.1 and/or Kv3.4 (Goldman-Wohl *et al.* 1994; Weiser *et al.* 1994), and Kv3 channels contribute to repolarization of both somatic Na^+ spikes and dendritic Ca^{2+} spikes (McKay & Turner, 2004). Genetic elimination of Kv3.3 subunits may be insufficient to exhibit the dendritic shrinkage and severe ataxia phenotypes because of functional compensation by Kv3.1 and Kv3.4 in PCs (Goldman-Wohl *et al.* 1994; Weiser *et al.* 1994; Martina *et al.* 2003). We detected the expression of Kv3.4 subunits in cultured PCs (Supplemental Fig. S3*D*). It is therefore reasonable to hypothesize that R424H mutant subunits form heteromultimeric channels not only with endogenous mKv3.3 but also with other members of Kv3.3, including Kv3.4, resulting in total inhibition of the K^+ channel activity in PCs. This may account for the differences in the morphological phenotypes of PCs in our results *versus* the knockout mice.

Zebrafish expressing infant-onset mutant zebrafish Kv3.3 (homologous to the F448L mutant in SCA13 patients) in spinal motoneurons show defective axonal pathfinding (Issa *et al.*, 2012). Indeed, the zebrafish is an interesting model for understanding the effects of mutant Kv3.3 expression in spinal motoneurons. However, as they used a motoneuron-specific enhancer of *Mnx1* (*Hb9*) gene, the exogenous proteins were not expressed in the cerebellar neurons. To examine the effects of mutant Kv3.3 in the cerebellum, it would be necessary to express the mutant protein directly in the cerebellar neurons using a different method.

Comparison of our culture results with SCA13 patients harbouring the R423H mutation

Spinocerebellar ataxia type 13 patients harbouring the R423H mutation generally show early-onset, slow-progressive ataxia and cerebellar atrophy (Figueroa *et al.* 2010, 2011). Our immunohistochemical analyses demonstrated that expression of R424H mutant subunits impaired dendritic development and induced cell death in cultured PCs (Figs 2 and 3). Those defects may be responsible for the cerebellar atrophy and ataxia observed in SCA13 patients, although it is necessary to verify that similar impairments are also observed in post-mortem cerebellum of the patients.

In functional aspects, we found that expression of R424H mutant subunits significantly decreased outward current mediated by voltage-gated K^+ channels, reduced sEPSCs, broadened action potentials and altered firing properties (Figs 4–7 and Table 2), suggesting the existence of similar functional changes in SCA13 patients. As PCs are the sole output neurons from the cerebellar cortex and make inhibitory synaptic contacts directly onto neurons in the deep cerebellar nuclei and the vestibular nuclei in the brainstem, PCs play crucial roles in motor co-ordination (Zheng & Raman, 2010). Accordingly, it is easily assumed that the reduction of spontaneous excitatory inputs and the changed firing properties in PCs disrupt synaptic transmission to neurons in the deep cerebellar nuclei and vestibular nuclei, resulting in impaired motor co-ordination. To examine the effects of the R424H mutation on electrophysiological properties of PCs and animal behaviour, we tried expressing R424H mutant subunits in PCs *in vivo* by directly injecting the virus solution into mouse cerebellar cortex as described in our previous papers (Torashima *et al.* 2006, 2008; Shuvaev *et al.* 2011). However, despite the presence of the infection, sufficient overexpression of mKv3.3 channels and apparent ataxia were not observed (data not shown). This may be because endogenous mKv3.3 proteins are abundantly expressed in PCs and the overexpression failed to reach the endogenous protein level. Efficient reduction of K^+ currents in PCs *in vivo* as observed in cultured PCs may be attained by using a different type of viral vector, such as adeno-associated virus vectors (Nathanson *et al.* 2009). Alternatively, K^+ currents in PCs *in vivo* may be effectively decreased using viral vector-mediated

expressions of R424H mutant subunits in *Kv3.3*$^{-/-}$ or *Kv3.3*$^{+/-}$ mice, which express no mKv3.3 proteins or only half the normal amount.

Currently, three different missense mutations in hKv3.3 channels have been reported from distinct pedigrees, and the disease onset and clinical phenotypes also differ among them (Waters *et al.* 2006; Figueroa *et al.* 2010, 2011). In the present study, we focused on only one mutation (R423H in hKv3.3) because of the drastic changes it induced in channel properties in the *Xenopus* oocyte expression system and its early-onset phenotype in SCA13 patients. Further studies of the effects of other mutants (R420H and F448L in hKv3.3) on cultured PCs may provide explanations for the differences in the disease phenotypes.

Possible significance of this study

We developed an *in vitro* SCA13 model using mouse cerebellar cultures and lentivirus vector-mediated gene expression. This model has advantages over *in vivo* models, such as transgenic mice, in the ease of controlling culture conditions by applying chemical compounds. Therefore, this model would be useful in screening drugs for SCA13 and in detailed investigations of the signalling cascades that promote the observed cell death. Given that blockade of P/Q-type Ca^{2+} channels rescued the phenotypes found in this research, the channel blockers may be potential therapeutic drugs for SCA13. Furthermore, this culture method, in combination with virus-mediated gene expression, may be applicable to the study of other types of hereditary spinocerebellar ataxia.

References

Armstrong CM & Bezanilla F (1974). Charge movement associated with the opening and closing of the activation gates of the Na channels. *J Gen Physiol* **63**, 533–552.

Ashcroft FM (2006). From molecule to malady. *Nature* **440**, 440–447.

Chang SY, Zagha E, Kwon ES, Ozaita A, Bobik M, Martone ME, Ellisman MH, Heintz N & Rudy B (2007). Distribution of Kv3.3 potassium channel subunits in distinct neuronal populations of mouse brain. *J Comp Neurol* **502**, 953–972.

Costa PF, Emilio MG, Fernandes PL, Ferreira HG & Ferreira KG (1989). Determination of ionic permeability coefficients of the plasma membrane of *Xenopus laevis* oocytes under voltage clamp. *J Physiol* **413**, 199–211.

Desai R, Kronengold J, Mei J, Forman SA & Kaczmarek LK (2008). Protein kinase C modulates inactivation of Kv3.3 channels. *J Biol Chem* **283**, 22283–22294.

Drummond GB (2009). Reporting ethical matters in *The Journal of Physiology*: standards and advice. *J Physiol* **587**, 713–719.

Erisir A, Lau D, Rudy B & Leonard CS (1999). Function of specific K^+ channels in sustained high-frequency firing of fast-spiking neocortical interneurons. *J Neurophysiol* **82**, 2476–2489.

Figueroa KP, Minassian NA, Stevanin G, Waters M, Garibyan V, Forlani S, Strzelczyk A, Bürk K, Brice A, Dürr A, Papazian DM & Pulst SM (2010). KCNC3: phenotype, mutations, channel biophysics—a study of 260 familial ataxia patients. *Hum Mutat* **31**, 191–196.

Figueroa KP, Waters MF, Garibyan V, Bird TD, Gomez CM, Ranum LP, Minassian NA, Papazian DM & Pulst SM (2011). Frequency of KCNC3 DNA variants as causes of spinocerebellar ataxia 13 (SCA13). *PLoS One* **6**, e17811.

Fry M, Boegle AK & Maue RA (2007). Differentiated pattern of sodium channel expression in dissociated Purkinje neurons maintained in long-term culture. *J Neurochem* **101**, 737–748.

Gillard SE, Volsen SG, Smith W, Beattie RE, Bleakman D & Lodge D (1997). Identification of pore-forming subunit of P-type calcium channels: an antisense study on rat cerebellar Purkinje cells in culture. *Neuropharmacology* **36**, 405–409.

Gimenez-Cassina A, Lim F & Diaz-Nido J (2007). Gene transfer into Purkinje cells using herpesviral amplicon vectors in cerebellar cultures. *Neurochem Int* **50**, 181–188.

Goldman-Wohl DS, Chan E, Baird D & Heintz N (1994). Kv3.3b: a novel Shaw type potassium channel expressed in terminally differentiated cerebellar Purkinje cells and deep cerebellar nuclei. *J Neurosci* **14**, 511–522.

Grynkiewicz G, Poenie M & Tsien RY (1985). A new generation of Ca^{2+} indicators with greatly improved fluorescence properties. *J Biol Chem* **260**, 3440–3450.

Hanawa H, Hematti P, Keyvanfar K, Metzger ME, Krouse A, Donahue RE, Kepes S, Gray J, Dunbar CE, Persons DA & Nienhuis AW (2004). Efficient gene transfer into rhesus repopulating hematopoietic stem cells using a simian immunodeficiency virus-based lentiviral vector system. *Blood* **103**, 4062–4069.

Harada KH, Ishii TM, Takatsuka K, Koizumi A & Ohmori H (2006). Effects of perfluorooctane sulfonate on action potentials and currents in cultured rat cerebellar Purkinje cells. *Biochem Biophys Res Commun* **351**, 240–245.

Hawley RG, Lieu FH, Fong AZ & Hawley TS (1994). Versatile retroviral vectors for potential use in gene therapy. *Gene Ther* **1**, 136–138.

Hille B (2001). *Ion Channels of Excitable Membranes*. Sinauer, Sunderland, MA.

Hirai H & Launey T (2000). The regulatory connection between the activity of granule cell NMDA receptors and dendritic differentiation of cerebellar Purkinje cells. *J Neurosci* **20**, 5217–5224.

Hirano T & Kasono K (1993). Spatial distribution of excitatory and inhibitory synapses on a Purkinje cell in a rat cerebellar culture. *J Neurophysiol* **70**, 1316–1325.

Hirano T, Kubo Y & Wu MM (1986). Cerebellar granule cells in culture: monosynaptic connections with Purkinje cells and ionic currents. *Proc Natl Acad Sci U S A* **83**, 4957–4961.

Hodgkin AL & Katz B (1949). The effect of sodium ions on the electrical activity of giant axon of the squid. *J Physiol* **108**, 37–77.

Hurlock EC, McMahon A & Joho RH (2008). Purkinje-cell-restricted restoration of Kv3.3 function restores complex spikes and rescues motor coordination in *Kcnc3* mutants. *J Neurosci* **28**, 4640–4648.

Issa FA, Mock AF, Sagasti A & Papazian DM (2012). Spinocerebellar ataxia type 13 mutation that is associated with disease onset in infancy disrupts axonal pathfinding during neuronal development. *Dis Model Mech* **5**, 921–929.

Joho RH, Street C, Matsushita S & Knöpfel T (2006). Behavioral motor dysfunction in Kv3-type potassium channel-deficient mice. *Genes Brain Behav* **5**, 472–482.

Kim JA, Kang YS, Jung MW, Kang GH, Lee SH & Lee YS (2000). Ca^{2+} influx mediates apoptosis induced by 4-aminopyridine, a K^+ channel blocker, in HepG2 human hepatoblastoma cells. *Pharmacology* **60**, 74–81.

Kubo Y & Murata Y (2001). Control of rectification and permeation by two distinct sites after the second transmembrane region in Kir2.1 K^+ channel. *J Physiol* **531**, 645–660.

Lajdova I, Chorvat D Jr, Spustova V & Chorvatova A (2004). 4-Aminopyridine activates calcium influx through modulation of the pore-forming purinergic receptor in human peripheral blood mononuclear cells. *Can J Physiol Pharmacol* **82**, 50–56.

McKay BE & Turner RW (2004). Kv3 K^+ channels enable burst output in rat cerebellar Purkinje cells. *Eur J Neurosci* **20**, 729–739.

MacKinnon R (1991). Determination of the subunit stoichiometry of a voltage-activated potassium channel. *Nature* **350**, 232–235.

Martina M, Yao GL & Bean BP (2003). Properties and functional role of voltage-dependent potassium channels in dendrites of rat cerebellar Purkinje neurons. *J Neurosci* **23**, 5698–5707.

Mellor JR, Merlo D, Jones A, Wisden W & Randall AD (1998). Mouse cerebellar granule cell differentiation: electrical activity regulates the $GABA_A$ receptor $\alpha 6$ subunit gene. *J Neurosci* **18**, 2822–2833.

Mikuni T, Uesaka N, Okuno H, Hirai H, Deisseroth K, Bito H & Kano M (2013). Arc/Arg3.1 is a postsynaptic mediator of activity-dependent synapse elimination in the developing cerebellum. *Neuron* **78**, 1024–1035.

Minassian NA, Lin MC & Papazian DM (2012). Altered Kv3.3 channel gating in early-onset spinocerebellar ataxia type 13. *J Physiol* **590**, 1599–1614.

Mintz IM & Bean BP (1993). Block of calcium channels in rat neurons by synthetic omega-Aga-IVA. *Neuropharmacology* **32**, 1161–1169.

Mullen RJ, Buck CR & Smith AM (1992). NeuN, a neuronal specific nuclear protein in vertebrates. *Development* **116**, 201–211.

Nathanson JL, Yanagawa Y, Obata K & Callaway EM (2009). Preferential labelling of inhibitory and excitatory cortical neurons by endogenous tropism of adeno-associated virus and lentivirus vectors. *Neuroscience* **161**, 441–450.

Orrenius S, Zhivotovsky B & Nicotera P (2003). Regulation of cell death: the calcium–apoptosis link. *Nat Rev Mol Cell Biol* **4**, 552–565.

Rae JL & Shepard AR (2000). Kv3.3 potassium channels in lens epithelium and corneal endothelium. *Exp Eye Res* **70**, 339–348.

Rudy B & McBain CJ (2001). Kv3 channels: voltage-gated K^+ channels designed for high-frequency repetitive firing. *Trends Neurosci* **24**, 517–526.

Sato M, Suzuki K, Yamazaki H & Nakanishi S (2005). A pivotal role of calcineurin signalling in development and maturation of postnatal cerebellar granule cells. *Proc Natl Acad Sci U S A* **102**, 5874–5879.

Sato Y, Sakaguchi M, Goshima S, Nakamura T & Uozumi N (2003). Molecular dissection of the contribution of negatively and positively charged residues in S2, S3, and S4 to the final membrane topology of the voltage sensor in the K^+ channel, KAT1. *J Biol Chem* **278**, 13227–13234.

Sawada Y, Kajiwara G, Iizuka A, Takayama K, Shuvaev AN, Koyama C & Hirai H (2010). High transgene expression by lentiviral vectors causes maldevelopment of Purkinje cells in vivo. *Cerebellum* **9**, 291–302.

Schilling K, Dickinson MH, Connor JA & Morgan JI (1991). Electrical activity in cerebellar cultures determines Purkinje cell dendritic growth patterns. *Neuron* **7**, 891–902.

Seoh SA, Sigg D, Papazian DM & Bezanilla F (1996). Voltage-sensing residues in the S2 and S4 segments of the *Shaker* K^+ channel. *Neuron* **16**, 1159–1167.

Sholl DA (1953). Dendritic organization in the neurons of the visual and motor cortices of the cat. *J Anat* **87**, 387–406.

Shuvaev AN, Horiuchi H, Seki T, Goenawan H, Irie T, Iizuka A, Sakai N & Hirai H (2011). Mutant PKCγ in spinocerebellar ataxia type 14 disrupts synapse elimination and long-term depression in Purkinje cells *in vivo*. *J Neurosci* **31**, 14324–14334.

Szymczak AL, Workman CJ, Wang Y, Vignali KM, Dilioglou S, Vanin EF & Vignali DA (2004). Correction of multi-gene deficiency in vivo using a single 'self-cleaving' 2A peptide-based retroviral vector. *Nat Biotechnol* **22**, 589–594.

Tabata T, Sawada S, Araki K, Bono Y, Furuya S & Kano M (2000). A reliable method for culture of dissociated mouse cerebellar cells enriched for Purkinje neurons. *J Neurosci Methods* **104**, 45–53.

Takayama K, Torashima T, Horiuchi H & Hirai H (2008). Purkinje-cell-preferential transduction by lentiviral vectors with the murine stem cell virus promoter. *Neurosci Lett* **443**, 7–11.

Torashima T, Iizuka A, Horiuchi H, Mitsumura K, Yamasaki M, Koyama C, Takayama K, Iino M, Watanabe M & Hirai H (2009). Rescue of abnormal phenotypes in $\delta 2$ glutamate receptor-deficient mice by the extracellular N-terminal and intracellular C-terminal domains of the $\delta 2$ glutamate receptor. *Eur J Neurosci* **30**, 355–365.

Torashima T, Koyama C, Iizuka A, Mitsumura K, Takayama K, Yanagi S, Oue M, Yamaguchi H & Hirai H (2008). Lentivector-mediated rescue from cerebellar ataxia in a mouse model of spinocerebellar ataxia. *EMBO Rep* **9**, 393–399.

Torashima T, Okoyama S, Nishizaki T & Hirai H (2006). In vivo transduction of murine cerebellar Purkinje cells by HIV-derived lentiviral vectors. *Brain Res* **1082**, 11–22.

Wang W, Xiao J, Adachi M, Liu Z & Zhou J (2011). 4-Aminopyridine induces apoptosis of human acute myeloid leukemia cells via increasing $[Ca^{2+}]_i$ through P_2X_7 receptor pathway. *Cell Physiol Biochem* **28**, 199–208.

Waters MF, Minassian NA, Stevanin G, Figueroa KP, Bannister JP, Nolte D, Mock AF, Evidente VG, Fee DB, Müller U, Dürr A, Brice A, Papazian DM & Pulst SM (2006). Mutations in voltage-gated potassium channel KCNC3 cause degenerative and developmental central nervous system phenotypes. *Nat Genet* **38**, 447–451.

Waters MF & Pulst SM (2008). SCA13. *Cerebellum* **7**, 165–169.

Weiser M, Vega-Saenz de Miera E, Kentros C, Moreno H, Franzen L, Hillman D, Baker H & Rudy B (1994). Differential expression of Shaw-related K^+ channels in the rat central nervous system. *J Neurosci* **14**, 949–972.

Zagha E, Manita S, Ross WN & Rudy B (2010). Dendritic Kv3.3 potassium channels in cerebellar Purkinje cells regulate generation and spatial dynamics of dendritic Ca^{2+} spikes. *J Neurophysiol* **103**, 3516–3525.

Zhao J, Zhu J & Thornhill WB (2013). Spinocerebellar ataxia-13 Kv3.3 potassium channels: arginine-to-histidine mutations affect both functional and protein expression on the cell surface. *Biochem J* **454**, 259–265.

Zheng N & Raman IM (2010). Synaptic inhibition, excitation, and plasticity in neurons of the cerebellar nuclei. *Cerebellum* **9**, 56–66.

Additional Information

Competing interests

None declared.

Author contributions

T.I. and H.H. conceived and designed experiments. T.I. and Y.M. performed experiments. T.I. collected and analysed data. T.I., Y.S. and H.H. wrote the paper.

Funding

This work was supported by Health Labour Sciences Research Grant (T.I.), JSPS KAKENHI grant numbers 24790230 (T.I.) and 19670003 (H.H.), and JSPS Funding Program for Next Generation World-Leading Researchers (LS021 to H.H.).

Acknowledgements

The lentiviral vector and MSCV promoter were provided by St Jude Children's Research Hospital and the American National Red Cross, respectively. We thank Dr L. K. Kaczmarek for mouse Kv3.3 cDNA and Dr K. Nakajo for technical advice and valuable comments on electrophysiological recording from *Xenopus* oocytes.

SUPPLEMENTAL FIGURE

Kv3.3 channels harboring a mutation of spinocerebellar ataxia type 13 alter excitability and induce cell death in cultured cerebellar Purkinje cells

Tomohiko Irie, Yasunori Matsuzaki, Yuko Sekino, and Hirokazu Hirai

Supplemental Fig. S1

Supplemental Figure S1. Amino acid sequence alignment of hKv3.3 (accession number AF022150) with the mKv3.3 used in this experiment

The two sequences were aligned using Clone Manager 6 software (Scientific & Educational Software, Cary, NC). Hyphens represent gaps introduced to optimize the alignment. The six transmembrane domains are surrounded by squares. Residues conserved between hKv3.3 and mKv3.3 are colored blue.

Supplemental Fig. S2

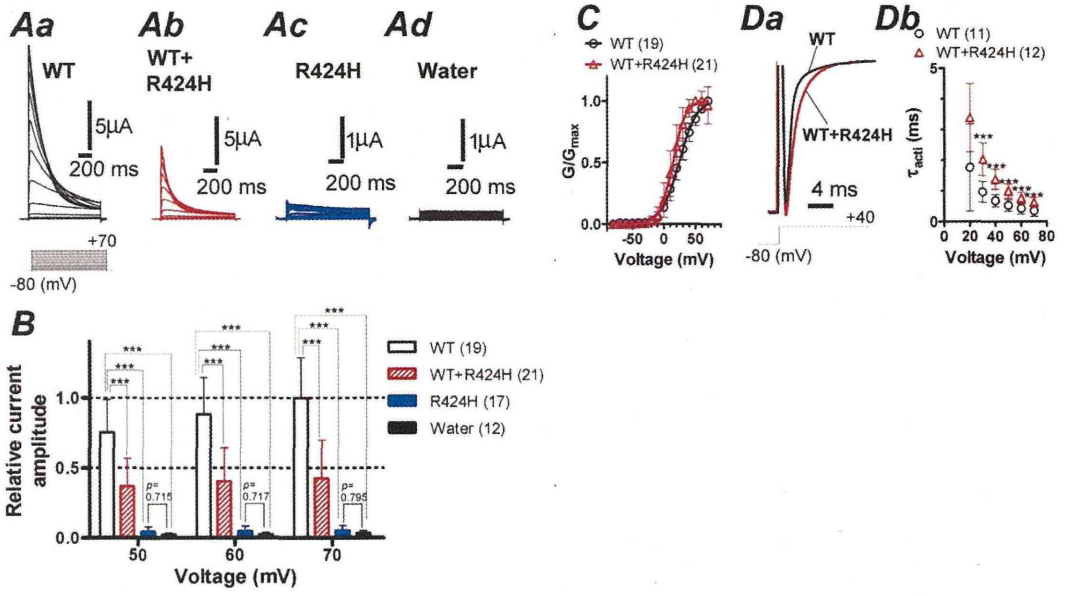

Supplemental Figure S2. R424H mutant subunits work as a dominant-negative on WT mKv3.3 channels expressed in *Xenopus* oocytes

A, Representative traces evoked by stepping from −80 mV holding potential to voltages ranging from −70 to +70 mV in 10-mV increments. cRNA of WT mKv3.3 (*Aa*, WT), a mixture of WT and R424H mutant subunits at 1:1 ratio (*Ab*, WT+R424H), R424H mutant subunits (*Ac*, R424H), or nuclease-free water (*Ad*, Water) was injected into *Xenopus* oocytes. *B*, Summary of the mean relative current amplitude. The amplitude was calculated from peak amplitude normalized by mean peak amplitude of WT-expressing oocytes at +70 mV voltage pulse. *C*, Normalized conductance (*G*) of WT-expressing and WT+R424H-expressing oocytes are plotted as a function of voltage. *G* was obtained by dividing peak current by electrochemical driving force: $[G = I_K/(V - E_K)]$. The activation (G/G_{max}) curves were fit with the Boltzmann function, $G/G_{max} = 1/ [1 + \exp (V_{1/2} - V)/k]$. *D*, Comparison of activation τ between WT-expressing and WT+R424H mutant-expressing oocytes. *Da*, Representative traces evoked by stepping from −80 mV holding potential to +40 mV. The current traces are scaled to the same peak amplitude to compare the activation kinetics. *Db*, Comparison of τ_{acti} of WT mKv3.3 with that of WT+R424H mutant channels in *Xenopus* oocytes. τ_{acti} was obtained by fitting current traces with a single exponential function on the rising phases of the traces.

Supplemental Fig. S3

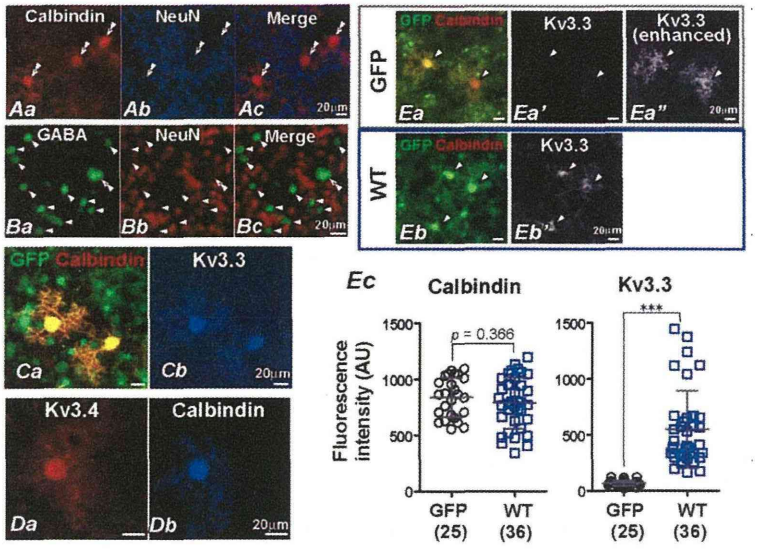

Supplemental Figure S3. Immunohistochemical characterization of mouse cerebellar cultures

A, Cerebellar cultures double-immunostained with anti-Calbindin and anti-NeuN antibodies at DIV 14. PCs (Calbindin-positive cells in *Aa*, double arrowheads) were NeuN-negative (*Ab* and *Ac*). *B*, Cultures double-immunostained with anti-GABA and anti-NeuN antibodies at DIV 16. GABAergic interneurons (GABA-positive small cells in *Ba* and *Bc*, arrowheads) were also NeuN-negative. Double arrowheads in *Ba* and *Bc* indicate a putative PC. *C*, Cultures triple-immunostained with anti-GFP, anti-Calbindin, and anti-Kv3.3 antibodies at DIV 14. PCs but not other cerebellar neurons expressed mKv3.3 channels. In *C*, GFP-expressing cerebellar cultures were used to visualize the neurons. *D*, Cerebellar cultures double-immunostained with anti-Kv3.4 and anti-Calbindin antibodies, showing the expression of Kv3.4 in PCs. *E*, Immunofluorescence images of cerebellar cultures infected with lentiviral vectors expressing GFP (*Ea-Ea"*) or WT subunits (*Eb* and *Eb'*). The cultures were double-immunostained with anti-GFP and anti-Kv3.3 antibodies. The fluorescence images were taken in the same conditions for the quantitative analysis. PCs are indicated by arrowheads. Panel *Ea"* is a contrast-enhanced image of *Ea'* that shows faint but some expression of endogenous mKv3.3 in PCs expressing GFP alone. *Ec*, Quantitative analysis of immunofluorescence intensity for Calbindin and Kv3.3. AU, arbitrary unit. In *A-E*, The following primary and secondary antibodies were used. Primary antibodies: mouse monoclonal anti-Calbindin antibody (*A*, *C*, and *D*, 1:2,000-diluted, No.300, Swant; Bellinzona, Switzerland), mouse monoclonal anti-NeuN antibody (*A* and *B*, 1:2,000-diluted), and rabbit polyclonal anti-GABA antibody (*B*, 1:1,000-diluted, A2052; Sigma-Aldrich), guinea pig polyclonal anti-GFP antibody (*C* and *E*, 1:1,000-diluted), and rabbit polyclonal anti-Kv3.3 antibody [*C* and *E*, 1:2,000-diluted, APC-102; Alomone labs, Jerusalem, Israel; This antibody is raised from the peptide KSPITPGSRGRYSRDRAC corresponding with residues 701-718 of rat Kv3.3a channels, which have a sequence that is identical to 692-709 of the mKv3.3 channels (Chang *et al.*, 2007)]. Secondary antibodies: AF 568-conjugated goat anti-rabbit IgG antibody (3*A*), AF 680-conjugated goat anti-mouse IgG antibody (*A* and *D*), AF 488-conjugated goat anti-rabbit IgG antibody (*B*, A-11008; Invitrogen), AF 568-conjugated goat anti-mouse IgG antibody (*B*, *C* , and *E*, A-11031; Invitrogen), AF 488-conjugated goat anti-guinea pig IgG antibody (*C* and *E*), AF 680-conjugated goat anti-rabbit IgG antibody (*C* and *E*, A-21109; Invitrogen). All secondary antibodies were used at the concentration of 5 μg/ml. The incubation conditions were same as Fig. 2. For immunolabeling of Kv3.4 protein in cerebellar cultures (*D*), goat serum was excluded from the incubation buffer. Cerebellar cultures were immunolabeled with goat polyclonal anti-hKv3.4 antibody (1:500-diluted, sc-104343; Santa Cruz Biotechnology, Santa Cruz, CA) and mouse monoclonal anti-Calbindin antibody, and then with AF 568-conjugated donkey anti-goat IgG antibody (A-11057; Invitrogen). After blocking with the incubation buffer containing 10% normal goat serum, the cultures were further incubated with AF 680-conjugated goat anti-mouse IgG antibody.

Supplemental Fig. S4

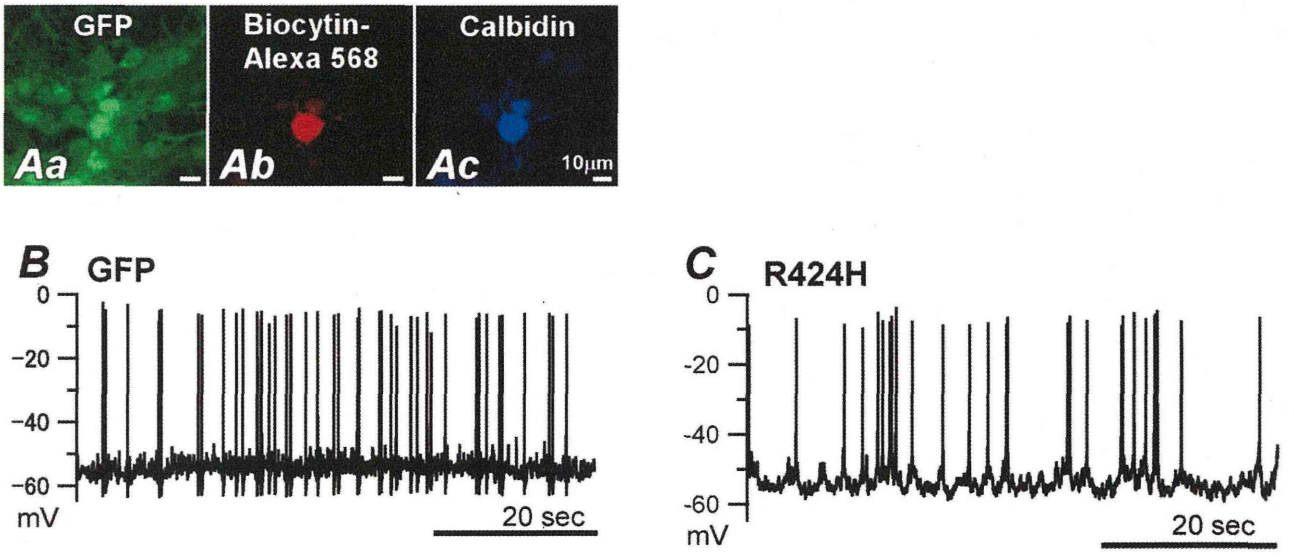

Supplemental Figure S4. Recordings of spontaneous action potentials from PCs

A, Immunohistochemical identification of PCs. PCs were stained intracellularly with biocytin infused via patch pipettes, fixed in 4% (w/v) formaldehyde, and incubated with mouse monoclonal anti-Calbindin antibody and guinea pig polyclonal anti-GFP antibody. The samples were further incubated with AF 568 streptavidin (S-11226, Invitrogen), AF 488-conjugated goat anti-guinea pig IgG antibody, and AF 680-conjugated goat anti-mouse IgG antibody. The incubation conditions were the same as in Fig. 2. *B* and *C*, Representative spontaneous firing recorded from GFP-expressing PC (*B*) and R424H mutant-expressing PC (*C*) at DIV 8.